*Int. J. Chem. Sci.: 12(1), 2014, 45-61*
*ISSN 0972-768X*
*www.sadgurupublications.com*

# IMAGING ELLIPSOMETRY STUDY ON THE EFFECT OF ELECTROLYTE ON THE DRAINAGE OF AN AQUEOUS FILM TRAPPED BETWEEN A PLANE HYDROPHILIC SILICA SURFACE AND AN APPROACHING ORGANIC DROPLET

**PARDON K. KUIPA[*a,b] and OLGA KUIPA[b]**

[a]School of Engineering and Technology, Chinhoyi University of Technology,
P. Bag 7724, CHINHOYI, ZIMBABWE
[b]Department of Chemical Engineering, National University of Science and Technology, BULAWAYO

## ABSTRACT

An imaging ellipsometer is used to study the drainage of an aqueous film trapped between a hydrophilic silica equilateral prism surface and a heptane or butylacetate droplet. The interfacial droplet profile on approach to the hydrophilic silica surface is such that the droplet is dimpled at its center with the periphery of the droplet (the barrier ring) being the region of closest approach to the hydrophilic silica surface. The time it takes for these drops to either achieve an equilibrium film thickness at the barrier ring or to coalesce with the macroscopic hydrophilic silica surface was experimentally determined; drainage time increases whilst equilibrium film thickness decreases with increasing salt concentration in the continuous phase. The increase in drainage time is attributed to hindered drainage of the aqueous film due probably to an increase in the aqueous film viscosity, which should translate into a decrease in the film elasticity. Compression of the double layer may also qualitatively explain the observed decrease in equilibrium film thickness at the barrier ring as the salt concentration increases. When aluminum chloride is used as the electrolyte the equilibrium film thickness is relatively constant (around 90 ± 10 nm) for the range of concentrations studied. This may be due to the fact that the aluminum ion has a valence of three and may screen electrostatic interactions between the oil droplet and the hydrophilic silica surface at relatively lower aluminum chloride concentrations.

**Key words**: Equilibrium film thickness, Film drainage, Film rupture, Imaging ellipsometer, Coalescence.

## INTRODUCTION

A fundamental understanding of the mechanism of thinning and rupture of the intervening film between colliding drops is important in understanding the mechanism of

[*]Author for correspondence; E-mail: kuipapardon@yahoo.com; Ph.: +263 67 29199; Fax: +263 67 29456

inter-drop coalescence. Mobility of the interface is dependent on physical parameters such as viscosity, density difference and elasticity. Coalescence is dependent on inter-droplet interactions, which can be related to the hydrodynamic forces, Brownian motion, London attractive forces, electrostatic repulsive forces and steric barriers due either to adsorbed surfactant molecules or to fine solids. For droplets (such as those in this study) with diameters much larger that 1 μm, Brownian motion has little effect on inter-droplet coalescence. Film drainage is generally governed by a combination of hydrodynamic and thermodynamic interactions[1]. When film thickness becomes smaller than 100 nm, surface forces which are short range by their nature, start to influence the film drainage process.

The study of coalescence of liquid drops driven by gravity at a flat interface provides a simple experimental setup that can be used to understand the effects of various physical parameters that contribute to the coalescence of drops in liquid-liquid as well as gas-liquid emulsions. If one considers coalescence between two drops or at a free interface the following steps leading to coalescence may be distinguished:

(i) Initial approach of the droplet to the interface. The interface deforms to a film as a result of the applied force and the interfacial tension. The shape of the deformed interface will depend on the interfacial tension between the droplet and the continuous phase, the capillary pressure inside the drops and the applied (buoyancy) force. A low value of the force will give rise to a flat circular interface while a large force might cause a concave dimple. Thus, if the film is established by the rapid approach of a bubble to a solid surface (as in this study), a substantial volume of the liquid is trapped in the centre of the film producing a dimple shaped draining film. The thin layer of liquid trapped within the deformed interface (film) drains out radially as a result of the force pressing the drops. This continues until the film thins to a critical value at which forces at the interfacial region such as the Van der Waals and electrostatic forces become important. The Van der Waals attraction force increases with decreasing film thickness. The Van der Waals forces cause the film to thin rapidly until rupture sets in.

(ii) When the film thickness reaches a critical value, the Van der Waals' attraction force becomes large enough to result in rupture (coalescence). Capillary instabilities may also cause rupture of the film leading to coalescence.

The study of coalescence in the presence of electrolyte or surfactant is important to the understanding and design of multi-phase contacting equipment. Several researchers have

studied the effect of electrolyte on film drainage. Blake and Kitchener[2] have shown that the equilibrium film thickness between an air bubble and a silica surface decreased with increasing electrolyte concentration and valency of the counter ion/cation. Hewitt et al.[3] confirmed these observations when they studied the drainage of an aqueous film trapped between an air droplet and a silica surface. They also observed that the drainage at the barrier ring increased significantly with increasing electrolyte concentrations whilst the drainage at the center of the film decreased with electrolyte concentration. These observations were explained in terms of the stabilizing effect of the double layer repulsion force between the surfaces. Thus, in aqueous solution, an oil droplet or an air droplet accumulates net negative charge. The silica surface is also negatively charged, so that electrostatic double layer repulsion is felt by the two approaching surfaces. The repulsive force acts to stabilize the system. An increase in electrolyte concentration reduces the range of the double layer repulsion due to charge neutralization or double layer compression, thus reducing the equilibrium film thickness. Equilibrium thickness is thus governed by double layer interaction between the drop and the silica surface as well as the drop and aqueous film hydrodynamics.

Lessard and Zieminski[4] and Marrucci and Nicodemo[5] have reported the effect of inorganic electrolytes on bubble coalescence in air-water systems. Their findings confirm that the presence of salts slows down the rate of film drainage. They also observed an abrupt increase in the coalescence time beyond a critical value of the salt concentration. Stevens et al.[6] and Chen et al.[7] have studied the rest times of oil droplets at an oil-water interface, in the presence of dissolved ionic electrolytes. They observed that the presence of salts did not significantly alter the rest times for non-polar droplets whilst a sharp increase in the rest times was observed for polar oils.

We have employed the technique of imaging ellipsometry[8-10] to study film drainage between an oil (heptane or butyl acetate) droplet that is immersed in an aqueous solution of varying salt (NaCl or aluminum chloride) concentration and a silica prism interface. Imaging ellipsometry is when a film thickness profile is obtained by imaging the reflected intensity over a given area with a digital CCD camera and then analyzing the film thickness spacially, resulting in the capture of a grey scale image and a profile of the film thickness. The lateral resolution of the grey scale image is defined by the pixel size of the CCD camera. Variation in the grey scale image is directly related to the variation in the intensity of reflected light. The image ranges from white corresponding to a very thick film to black corresponding to a very thin film. In this study, imaging ellipsometry is used due to its non-perturbation nature and its ability to sample a film profile in real time[11-13].

It was envisaged that the results of the study would add to the fundamental knowledge that is necessary for the design of liquid-liquid and gas-liquid contacting equipment.

## Apparatus

### Imaging ellipsometer

A modified imaging ellipsometer from Beaglehole Instrument was used to study film drainage and to profile droplet cross-sections. The imaging ellipsometer is a sensitive optical device for the determination of surface and thin film properties. It measures the changes in the state of polarization of light when it is reflected from a sample surface, thus the film thickness and the refractive index of an unknown medium are obtained.

A highly sensitive digital CCD camera is used as the detector to capture the intensity and ellipticity of the reflected light. The CCD image is digitised, which eliminates noise effects. The image is transferred to the computer via a frame grabber. In this study, a DVC-10 marquee camera (10 bits/pixel) was used. The detector has the active pixel area of 755 pixels on the horizontal (size = 7.95 μm) and 484 pixels (size = 7.5 μm) on the vertical. Therefore, with the lens magnification of 1.0, the corresponding sampling area of 6 mm × 3.63 mm on the sample is obtained, as defined by the 2-dimensional CCD array.

### Sample cell

In the present study, an experimental cell was made specifically to contain the system samples. The experimental cell, as can be seen in Figure 1, is made up of a cylindrical tube with an inner diameter of 280 mm and the tube is tapered at the base to the diameter of 120 mm. The top of the tube is grounded flat. An equilateral dispersing prism seals the top of the tube on an extended platform, which ensures the gas-tight condition for the sample cell. A cap with an aperture is screwed onto the base of the cell.

A capillary with an outer diameter of 1.0 mm is inserted into the sample cell through the aperture and is positioned 2 mm from the silica/aqueous interface. The capillary is connected to a gas-tight syringe (capacity of 1 mL), which is contained in a repeating dispenser. The repeating dispenser delivers 1/50 (20 μL) of the total volume on each actuation. Both the syringe and repeating dispenser were obtained from Hamilton Co, USA.

The whole sample cell is mounted to a support, which is secured on an optical jack fitted with an x-y translator. The sample cell support, optical jack and translator are mounted on an anti-vibration table to ensure the elimination of all vibration during the operation of rotating arms, droplet expansion and other external disturbances.

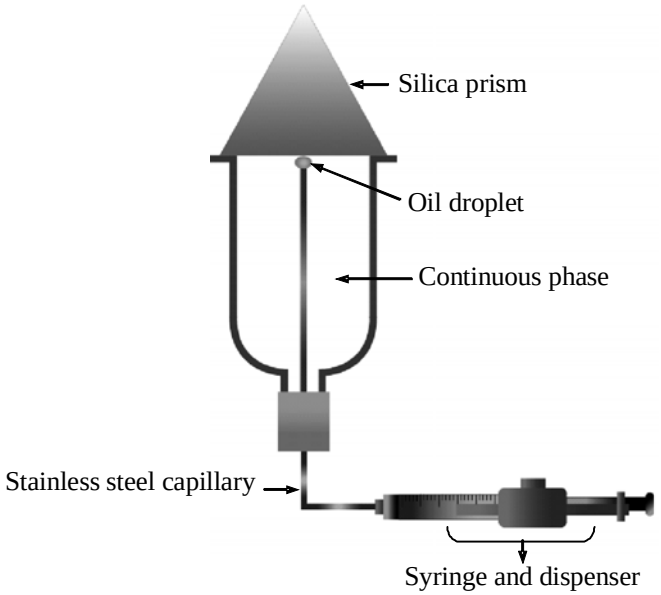


**Fig. 1: Schematic diagram of the sample cell employed in film drainage measurement**

## EXPERIMENTAL

### Materials

The sodium and aluminum chlorides had minimum purities of 99.9% and 99% and were obtained from Rhone-Poulenc and Sigma-Aldrich, respectively. The butyl acetate was of HPLC grade with a minimum purity of 99.7% and was obtained from Sigma Aldrich. Heptane was of Anala R grade with a minimum purity of 99%. The water used in the experiment for all the solution is produced using the Milli-Q™ filtration system. This filtration system purifies the water by removing dissolved organic impurities, residual chloride and inorganic electrolytes. The purified water has a conductivity of 0.055 μS/cm and surface tension of 72.8 mN/m at 21°C.

### Hydrophilic silica surface

The silica substrate used in this study is suprasil, supplied by Ealing Optics. Chemically, the silica surface structure is in either of the two forms, which are a siloxane group (≡Si-O-Si≡) or a silanol group (≡Si-OH). Three different types of silanol (free silanols, vicinal silanols and geminal silanols) are found and their distributions of hydroxyl groups on a silica surface determine the molecular adsorption behaviour on the surface[14].

When the silica surface is fully hydroxylated, it is able to adsorb water physically by means of hydrogen bonding. This type of surface is termed hydrophilic. Details for rendering a silica surface to fully hydrophilic are given below.

## Procedures

### Cleaning procedures

### Silica prism surface

The silica prism and lead glass used in this study were cleaned of surface contaminants by first lightly scrubbing with a warm solution of Extran 100 from Merck and then thoroughly rinsed with Milli-Q™ water. In order to render the silica surface fully hydrophilic, the silica prism was treated with a warm ammonium peroxide solution, which was prepared by mixing 2 parts hydrogen peroxide and 1 part of Milli-Q™ water and then adding a small aliquot of ammonia solution. The prism was then rinsed thoroughly with Milli-Q™ water and immersed in the Milli-Q™ water in a sealed container prior to use. This was to ensure the surface remained hydrophilic and prevent impurities from the surrounding to adsorb into the silica surface.

### Capillaries and glassware

The stainless steel capillary used in this study was first soaked in Extran 100 solution for 12 hrs, followed by copious rinsing with Milli-Q™ water. It was then flushed with and immersed in a nitric acid bath for 2 hrs, followed by repeated rinsing and flushing with Milli-Q™ water. The clean capillary was then dried in a clean oven for approximately 24 hours prior to use.

All the other fittings and glassware, including the syringe and glass cell were washed in Extran 100 solution for 2 hrs before copious rinsing with Milli-Q™ water. They were then soaked in concentrated sodium hydroxide solution for 2 hours then again rinsed with Milli-Q™ water.

### Measurement of droplet profiles

The cylindrical tube described above was first placed horizontally at the ellipsometer measurement axis. Then, the stainless steel capillary was inserted through the base of the cylindrical tube and positioned at a distance of 2.2 mm from the cell rim. Then, the sample cell was filled with the continuous phase and the silica prism was placed to seal the top of the sample cell. The silica prism was positioned to ensure the alignment of the optical

components of the ellipsometer. By adjusting the height of the sample cell, using the optical jack, a maximum intensity at the centre of the grabber in the computer screen, as monitored by the image, was obtained.

The intensity of the incident light was determined by measuring the intensity of the light reflected from the sample surface without the droplet at the critical angle, as determined from Snell's Law at a fixed light exposure. At this angle, all incident light on the fresh sample is fully reflected back into the incident medium.

In reflectometry studies, the angle of incidence is important to obtain the highest possible intensity of reflected light from the interface. Consider the case of an oil droplet approaching a silica surface in the continuous phase. As shown in Fig. 2, the incident light is reflected and refracted continuously at interfaces of silica-continuous phase, continuous phase-oil droplet and continuous phase-silica. The proportion of light reflected and refracted at each interface is dependent on the incidence angle and the refractive indices.

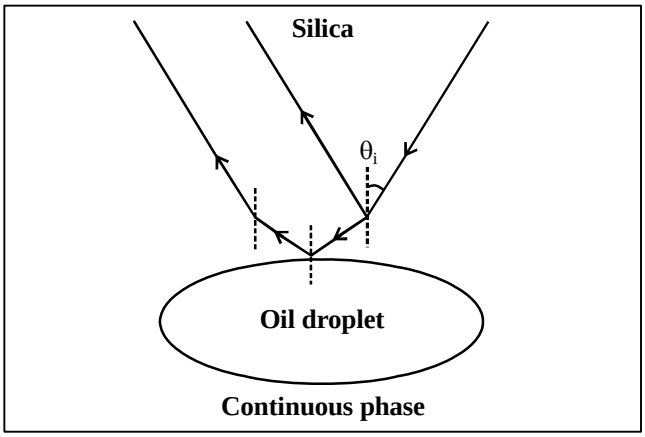


**Fig. 2: Reflection and transmission at interfaces of the optical system studied. $\theta_i$ is the angle of incidence at the silica-continuous phase interface**

The proportion of the total reflection from all interfaces to the incident light is determined by calculating the reflectance and transmittance at each interface, using the Fresnel reflection coefficients. This is done for the system here using refractive indices for silica, butyl acetate and the continuous phase (water) of 1.458, 1.3941 and 1.3333 respectively. Fig. 3 contains a plot of the percent of reflected light calculated for the p and s components for the optical system consisting of silica, continuous phase (water) and oil, as shown in Fig. 2.

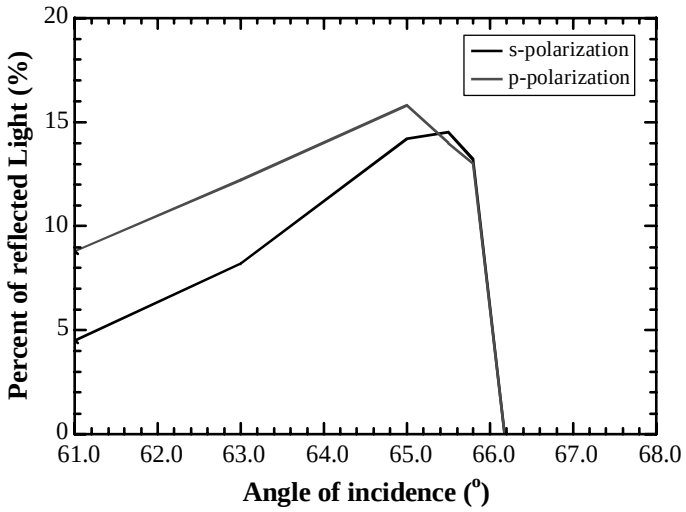


**Fig. 3: Percent of reflection for p and s polarisation as a function of angle of incidence at silica-continuous phase interface, for reflection from the three-phase system in Fig. 2**

It is clear from Fig. 3 that, for the optical system studied here the percentage of reflected intensity for the p and s components of the reflected light display a maximum at an angle of incidence of 65-65.5°. Thus, reflection is maximised at this angle of incidence (also known as the Brewster angle) when monitoring reflectivity for the optical system of interest.

Before formation of an oil droplet, an image of the background noise is taken. The oil droplet is then formed by actuation of the repeating dispenser. The measurements of the intensity of the light reflected from the droplet are initially taken at intervals of 10 seconds for the slow drainage processes studied here. Gradually the intervals are increased when the film drainage starts to slow down until equilibrium is reached. The total reflectance can be determined by:

$$R_f = \frac{I_r - I_{rb}}{I_i - I_{ib}}$$

where $I_r$ and $I_{rb}$ are the intensity of light reflected from the droplet surface and intensity of background noise respectively, and $I_i$ and $I_{ib}$ are the intensity of light reflected at incidence angle (total reflection) and intensity of background noise at incidence angle, respectively.

Ellipsometry measurements are performed in a similar manner to the reflectometry

measurements, as described previously. In ellipsometry, the ellipticity signal is most sensitive at the Brewster angle, $\theta_B$, viz:

$$\tan^{-1}\theta_B = \frac{n_3}{n_1}$$

where $n_1$ and $n_3$ are the refractive indices of the ambient (silica) and the substrate (droplet phase), respectively. However, a large error normally occurs when carrying out ellipsometry measurements[8]. Thus, in this study, the ellipsometry measurements are carried at 2-3° lower than the Brewster angle to minimise the error[8].

Typically, in the imaging ellipsometry/reflectometry experiments, the reflected signal gives a grey-scale image. In the analysis of this grey-scale image, a film profile is obtained by taking a cross-section through the image and calculating the film thickness along the cross section.

## RESULTS AND DISCUSSION

The oil droplet adopts a dimpled profile on approach to the silica/aqueous interface. The typical grey scale images of the oil droplet for the butyl acetate system are shown in Figures 4 and 5. In these images the white/lighter regions correspond to areas where the film thickness is thick. The images become darker the thinner the film. In the images shown in these figures the droplet is deformed such that it is dimpled at its centre with the periphery of the droplet (the barrier ring) being the region of closest approach of the droplet to the surface. It is also evident in these images that the system without salt has a thicker equilibrium film thickness than the system with salt (grey image for the system without salt at equilibrium as opposed to a black image for the system with salt at equilibrium). The images recorded for the system with electrolyte in the aqueous phase appear to show aggregates (perhaps crystals) within the aqueous film (see images after t = 3600 seconds). Formation of aggregates at the interface can result in a substantial increase in surface viscosities resulting in hindered drainage of the interfacial aqueous film. The dimpling of a droplet is typically attributed to non-uniform drainage of the film confined by the droplet and the silica surface[15,16]. The following mechanism is believed to contribute to this non-uniform drainage. On initial approach of the oil droplet to the silica surface, the spherical shape of the droplet determines the film profile. The film at the periphery of the drop is relatively thick compared to that at the center of the drop since the drop's center corresponds to the point of closest approach to the surface. A small viscous drag force as compared to the inner center of the drop opposes initial drainage from the periphery of the film. The film at the drop's center experiences

hindered flow compared to the film's periphery. The difference in the rate of film drainage across the drop leads to a build up of fluid at the film's center and the drop dimples as a result.

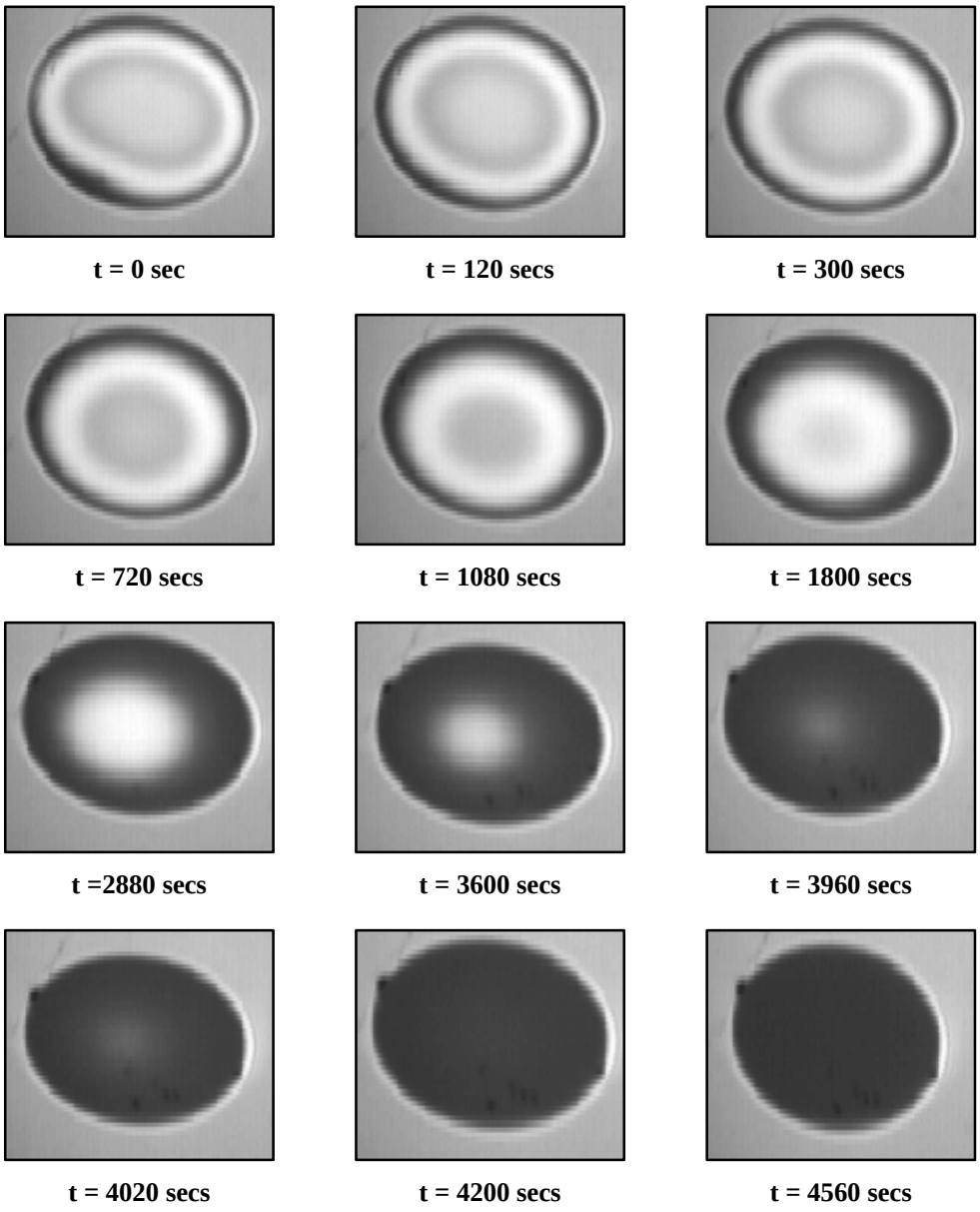


**Fig. 4: Reflectometry images for the butyl acetate/0.0001 M NaCl system showing dimple evolution with time**

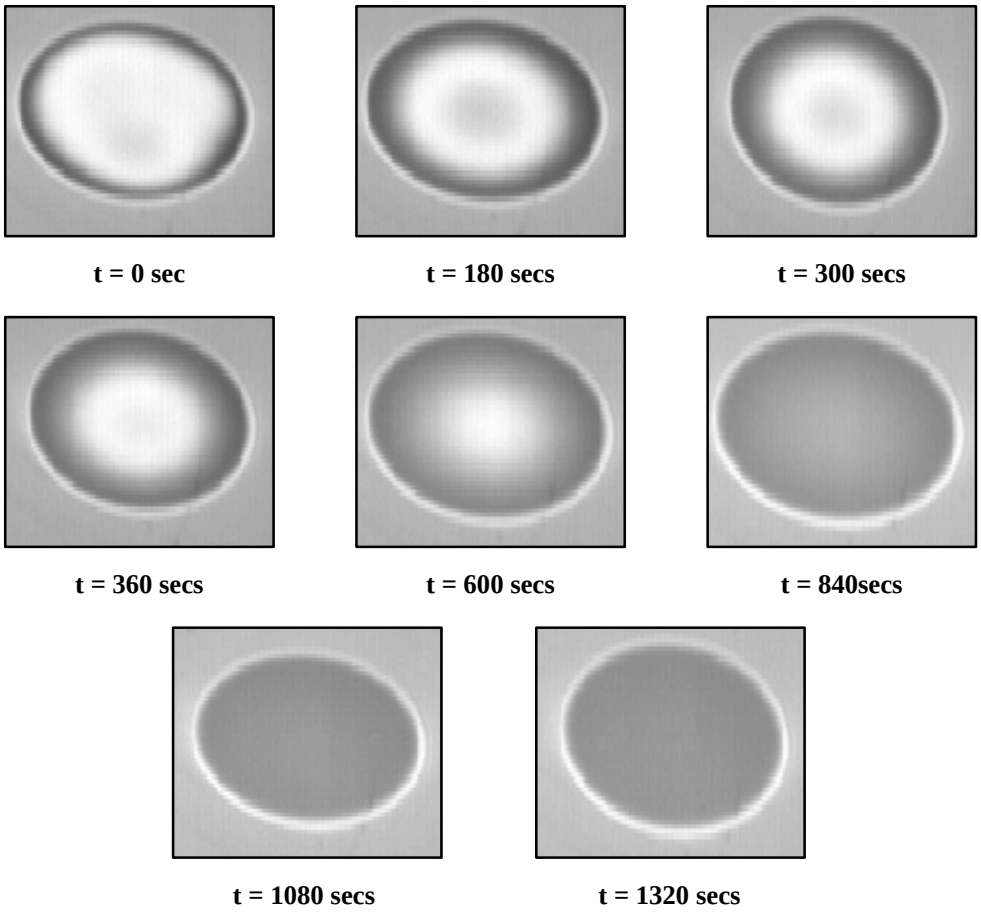


**Fig. 5: Reflectometry images for the butyl acetate/water system showing dimple evolution with time**

In all cases a stable, finite film thickness is formed with time at the barrier ring. This implies that there is a positive disjoining pressure stabilizing the film. The positive disjoining pressure is as a result of a significant repulsive force between the drop and the surface in the aqueous continuous phase opposing any further thinning of the film. The repulsive force is attributable to a repulsive double layer interaction between the droplet and the solid surface. The double layer repulsion is a result of the similar negative charge at the two approaching surfaces. The initial film profile observed in this work seems to suggest that there is oscillation at the interface, which dampens at times around 1000 seconds when a single dimple forms. The oscillations are thought to be hydrodynamic in nature due to the low viscosity of the oil phases that were used in this work. The film thickness at the drop centre does not seem to follow a rule (Figs. 6, 7, 9 and 12) may be due to the oscillation at the interface described above.

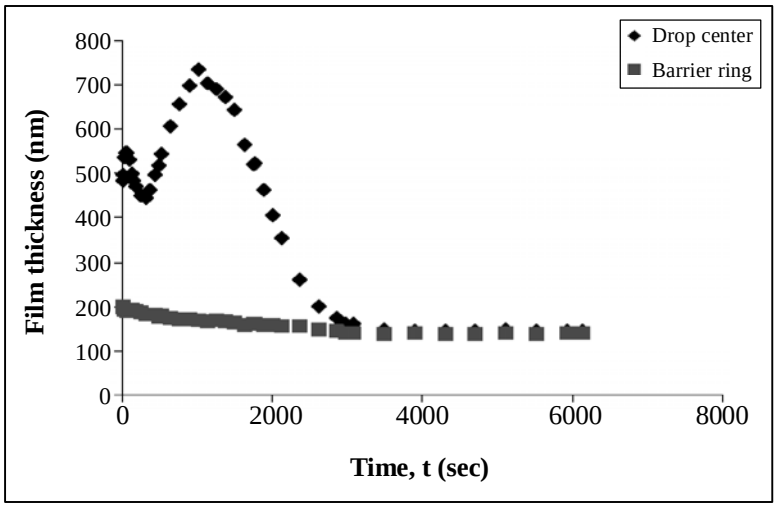


**Fig. 6: Evolution of film thickness at the drop centre and barrier ring for an aqueous film containing 0.0001M NaCl and trapped between a silica hydrophilic surface and a heptane droplet**

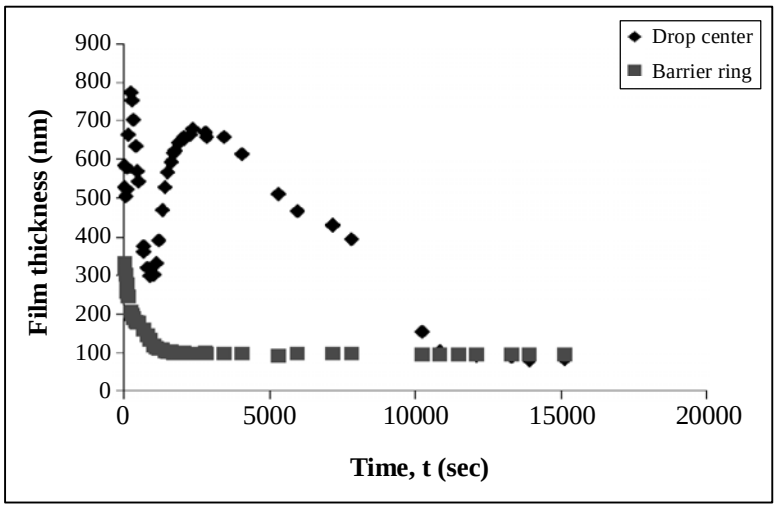


**Fig. 7: Evolution of film thickness at the drop centre and barrier ring for an aqueous film containing 0.0001 M NaCl and trapped between a silica hydrophilic surface and a butyl acetate droplet**

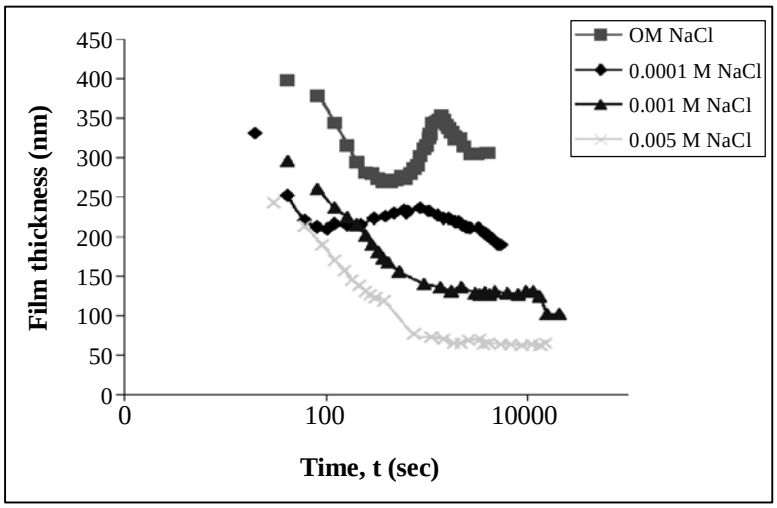


**Fig. 8: Evolution of film thickness at the barrier ring for an aqueous film of varying NaCl concentration and trapped between a silica hydrophilic surface and a butyl acetate droplet**

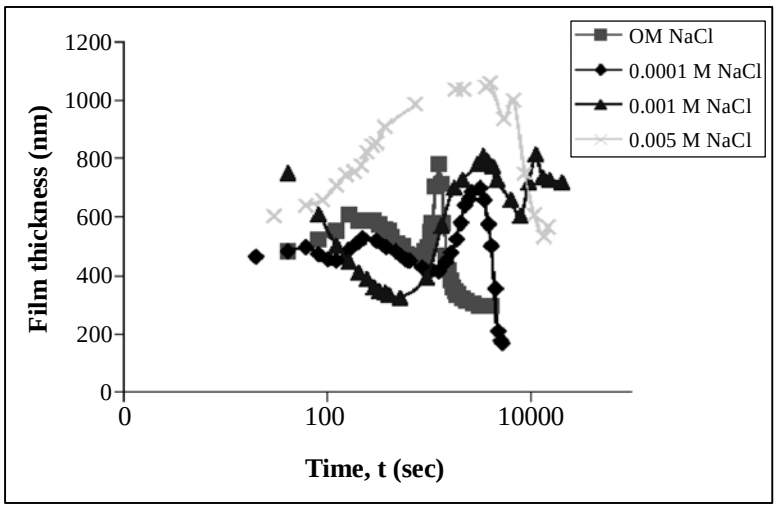


**Fig. 9: Evolution of film thickness at the drop centre for an aqueous film of varying NaCl concentration and trapped between a silica hydrophilic surface and a butyl acetate droplet**

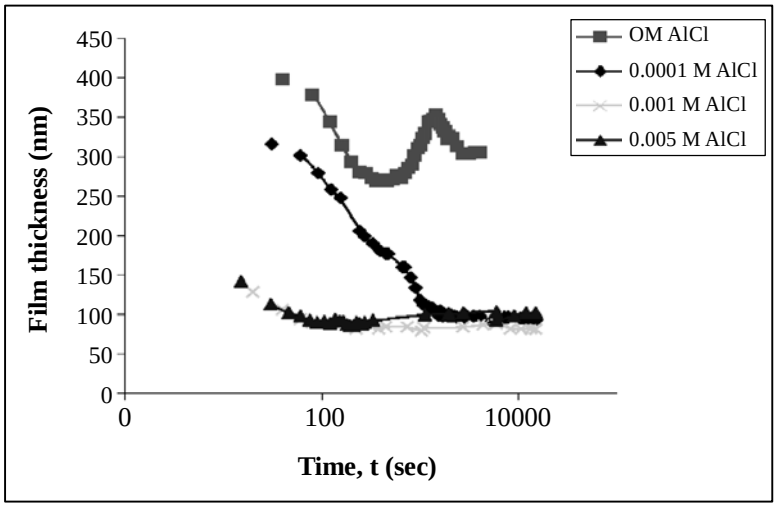


**Fig. 10: Evolution of film thickness at the barrier ring for an aqueous film of varying $AlCl_3$ concentration and trapped between a silica hydrophilic surface and a butyl acetate droplet**

The film drainage rates for the butyl acetate/NaCl and butyl acetate/aluminum chloride systems are shown in Figures 7 to 10. In the former system, there is a clear decrease in equilibrium film thickness as the salt concentration increases so that for 0, 1 x $10^{-4}$, 1 x $10^{-3}$ and 5 x $10^{-3}$ M NaCl the corresponding equilibrium film thicknesses are 304 nm, 190 nm, 130 nm and 62 nm, respectively. In the latter system it seems that the equilibrium film thickness is of the same order of magnitude for the whole range of salt concentrations studied in this study (around 90 nm) and differs markedly from the case when no salt is present. This may be explained by the fact that the aluminum ion has a valence of three and may screen electrostatic interactions between the oil droplet and the hydrophilic silica surface at relatively lower salt concentrations than those employed in this study. The sudden decrease in film thickness from 130 nm to about 102 nm for the 1 x $10^{-3}$ M case may be due to a sudden collapse of the equilibrium film thickness either due to some impurity in the system or to some other phenomenon.

The film drainage rates for the heptane/NaCl and heptane/aluminum chloride systems are shown in Figures 6 and Figures 11 to 13. In the former system, there is a clear decrease in equilibrium film thickness as the salt concentration increases so that for 0, 1 x $10^{-4}$, 1 x $10^{-3}$ and 5 x $10^{-3}$ M NaCl the corresponding equilibrium film thicknesses are 186 nm, 139 nm, 102 nm and 87 nm, respectively. In the latter system, it seems that the equilibrium film thickness is of the same order of magnitude for the whole range of salt concentrations studied in this work (90 ± 10 nm) and differs markedly from the case when

no salt is present. The sudden decrease in film thickness from 90 nm to about 40 nm for the 1 x $10^{-4}$ and 1 x $10^{-3}$ M cases may be due to a sudden collapse of the equilibrium film thickness either due to some impurity in the system or to some other phenomenon.

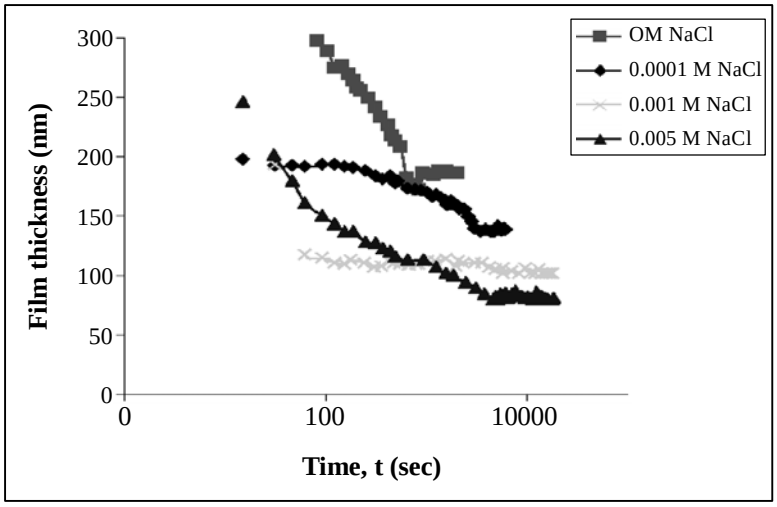


**Fig. 11: Evolution of film thickness at the barrier ring for an aqueous film of varying NaCl concentration and trapped between a silica hydrophilic surface and a heptane droplet**

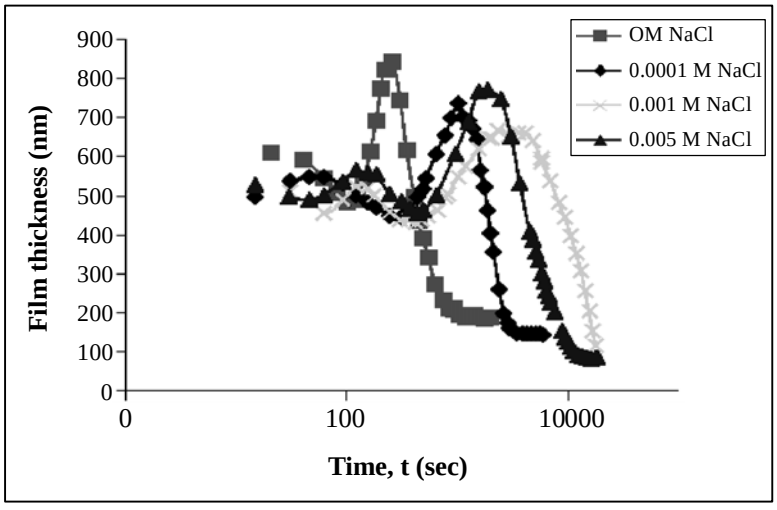


**Fig. 12: Evolution of film thickness at the drop centre for an aqueous film of varying NaCl concentration and trapped between a silica hydrophilic surface and a heptane droplet**

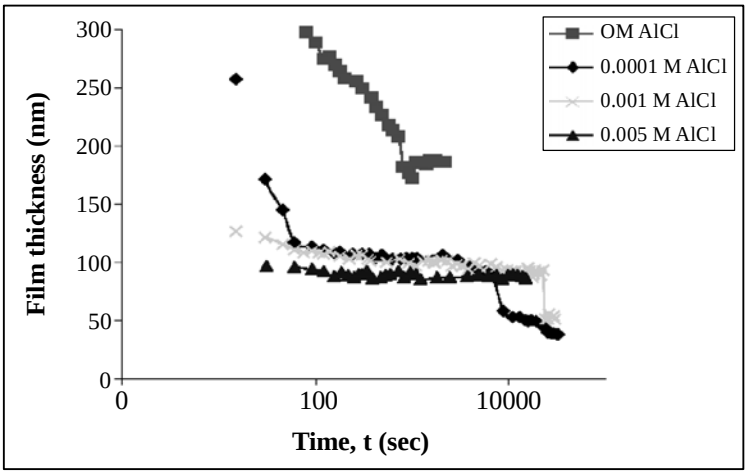


**Fig. 13: Evolution of film thickness at the barrier ring for an aqueous film of varying $AlCl_3$ concentration and trapped between a silica hydrophilic surface and a heptane droplet**

## CONCLUSION

The film thickness at the barrier ring decreases with increasing electrolyte concentration so that drainage of fluid from the film center is hindered. As a consequence, higher drainage times are observed as the salt concentration increases before an equilibrium film thickness at the barrier ring is achieved. The differences observed between sodium chloride and aluminum chloride as the electrolyte are attributable to the higher valence of the aluminum ion. Liquid drains more slowly for the case where aluminum chloride is used as electrolyte probably due to the fact that the more strongly adsorbed aluminum ion at the solid/liquid interface increases surface elasticity and viscosity of the interfacial film and consequently its mobility.

## REFERENCES

1. B. Derjaguin and M. Kussakov, Anomalous Properties of Thin Polymolecular Films V. An Experimental Investigation of Polymolecular Solvate (Adsorbed) Films as Applied to the Development of a Mathematical Theory of the Stability of Colloids, Acta Physicochimica USSR, **10(1)**, 25 (1939).
2. T. D. Blake and J. A. Kitchener, Stability of Aqueous Films on Hydrophobic Methylated Silica, J. Chem. Soc., Faraday Trans., **68**, 1435 (1972).
3. D. Hewitt, D. Fornasiero, J. Ralston, Aqueous Film Drainage at the Quarz/Water/Air Interface, J. Chem. Soc., Faraday Trans., **89(5)**, 817 (1993).

4. R. R. Lessard, S. A. Zieminski, Bubble Coalescence and Gas Transfer in Aqueous Electrolytic Solutions, Ind. Eng. Chem. Fundam., **10**, 260 (1971).

5. G. Marrucci, L. Nicodemo, Coalescence of Gas Bubbles in Aqueous Solutions of Inorganic Electrolytes, Chemical Engineering Science, **22**, 1257 (1967).

6. G. W. Stevens, H. R. C. Pratt and D. R. Tai, Droplet Coalescence in Aqueous Electrolyte, Solutions, J. Colloid Interface Sci., **136**, 470 (1990).

*7.* Chao-Tai Chen, Jer-Ru Maa, Yu-Min Yang and Chien-Hsiang Chang, Effects of Electrolytes and Polarity of Organic Liquids on the Coalescence of Droplets at Aqueous-organic Interfaces, **406(1-3)**, 167 (1998).

8. Beaglehole Instruments, Imaging Ellipsometer Manual, Version 4.7 (2003).

9. R. M. A. Azzam and N. M. Bashara, Ellipsometry and Polarized Light, North Holland Inc., New York (1977).

10. D. Beaglehole, Inadequacy of the Lifshitz Theory for Thin Liquid Films, Phys. Rev. Letters, **66(16)**, 2084 (1991).

11. D. G. Goodall, M. L. Gee, G. W. Stevens, J. Perera and D. Beaglehole, An Investigation of the Critical Thickness of Film Rupture and Drainage Phenomena using Dual Wavelength Ellipsometry, Coll. Surf. A, **143**, 41 (1998).

12. M. Schneider, U. Langklotz and A. Michaelis, Thicknesss Determination of Thin Anodic Titanium Oxide Films-a Comparison Between Coulometry and Reflectometry, Surface and Interface Analysis, **43(12)**, 1471 (2011).

13. D. G. Goodall, M. L. Gee and G. W. Stevens, An Imaging Reflectometry Study of the Effect of Electrolyte on the Drainage and Profile of an Aqueous Film Between an Oil Droplet and a Hydrophilic Silica Surface, Langmuir, **18(12)**, 4729 (2002).

14. E. E. Vansant, P. V. D. Voort and K. C. Vrancken, Characterization and Chemical Modification of the Silica Surface, Elsevier Science, Amsterdam (1995).

15. S. Hartland, The Coalescence of a Liquid Drop at a Liquid-liquid Interface, Part II, Film Thickness, Trans, IChemE., **45**, T102 (1967).

16. R. S. Allan and S. G. Mason, Effects of Electric Fields on a Coalescence in Liquid-Liquid Systems, Trans, Faraday Soc., **57**, 2027 (1961).

*Accepted : 22.11.2013*